

SCIENTIFIC REPORTS



OPEN

Heterologous Expression of a Novel Drug Transporter from the Malaria Parasite Alters Resistance to Quinoline Antimalarials

Sarah M. Tindall¹, Cindy Vallières¹, Dev H. Lakhani¹, Farida Islahudin², Kang-Nee Ting³ & Simon V. Avery¹ 

Antimalarial drug resistance hampers effective malaria treatment. Critical SNPs in a particular, putative amino acid transporter were recently linked to chloroquine (CQ) resistance in malaria parasites. Here, we show that this conserved protein (PF3D7_0629500 in *Plasmodium falciparum*; AAT1 in *P. chabaudi*) is a structural homologue of the yeast amino acid transporter Tat2p, which is known to mediate quinine uptake and toxicity. Heterologous expression of PF3D7_0629500 in yeast produced CQ hypersensitivity, coincident with increased CQ uptake. PF3D7_0629500-expressing cultures were also sensitized to related antimalarials; amodiaquine, mefloquine and particularly quinine. Drug sensitivity was reversed by introducing a SNP linked to CQ resistance in the parasite. Like Tat2p, PF3D7_0629500-dependent quinine hypersensitivity was suppressible with tryptophan, consistent with a common transport mechanism. A four-fold increase in quinine uptake by PF3D7_0629500 expressing cells was abolished by the resistance SNP. The parasite protein localised primarily to the yeast plasma membrane. Its expression varied between cells and this heterogeneity was used to show that high-expressing cell subpopulations were the most drug sensitive. The results reveal that the PF3D7_0629500 protein can determine the level of sensitivity to several major quinine-related antimalarials through an amino acid-inhibitable drug transport function. The potential clinical relevance is discussed.

The fight for malaria eradication continues apace, but there were still over 200 million cases of this devastating parasitic disease in 2015^{1,2}. In the absence of a commercially available vaccine, artemisinin combination therapies (ACTs) are the current main line of antimalarial defence in most countries. Quinoline antimalarials (commonly in combination with an antibiotic) are also recommended as first-line malaria treatments during early pregnancy and second line treatment for uncomplicated malaria cases, but remain first line drugs in many African countries³⁻⁵. Furthermore, quinoline derivatives such as amodiaquine, mefloquine and lumefantrine are currently used in recommended ACTs. Chloroquine was one of the most effective drugs ever produced and, along with primaquine, remains a drug of choice for treating *Plasmodium vivax* malaria⁵. Quinine (QN) has historically been a mainstay of the antimalarial drug repertoire but the wider use of QN is now hampered by poor compliance, the prevalence of adverse drug reactions and the availability of alternative antimalarials³.

One strategy in the battle against malaria is the identification of drug resistance mechanisms in the parasite. Identifying genetic changes that confer drug resistance helps the spread of resistance to be tracked and can allow appropriate antimalarial drug therapy to be tailored^{6,7}. In addition, knowledge of the genetic basis for resistance can give insight to the mechanism of action of a drug, informing improved drug design or treatment strategies. Membrane transporters provide a classic example of proteins that can mediate drug resistance or sensitivity^{8,9}. In the malaria parasite most lethal to humans, *Plasmodium falciparum*, multiple transporters have been associated with altered sensitivity to quinoline antimalarials including PfCRT, PfNHE1, PfMDR1 and PfMRP¹⁰. PfCRT is the most widely reported of these, localized to the parasite digestive vacuole and in which SNPs are commonly

¹School of Life Sciences, University of Nottingham, University Park, Nottingham, NG7 2RD, UK. ²Faculty of Pharmacy, Universiti Kebangsaan, Kuala Lumpur, 50300, Malaysia. ³Department of Biomedical Sciences, University of Nottingham Malaysia Campus, Semenyih, Malaysia. Sarah M. Tindall and Cindy Vallières contributed equally to this work. Correspondence and requests for materials should be addressed to S.V.A. (email: Simon.Avery@nottingham.ac.uk)

associated with chloroquine resistance¹¹. Quinine resistance took over 200 years to emerge, but this is in striking contrast to other antimalarial drugs. Widespread resistance to chloroquine was evident just 40 years after its introduction. Quinine resistance is only found in some malaria-endemic areas and is usually low level³. The incidence of chloroquine resistance may sometimes be reversed relatively quickly when chloroquine treatment is discontinued^{12,13}. Therefore, in the face of rising ACT resistance¹⁴ quinolines could in some regions continue to provide a valid alternative in the future.

One problem with characterisation of drug transport and resistance mechanisms in malaria parasites is that not all of the relevant species are easy to cultivate in the laboratory or to manipulate genetically, although improvements are being made including with *P. falciparum*^{15,16}. Model organisms may be exploited as an alternative. The yeast *Saccharomyces cerevisiae* is an especially powerful model of eukaryotic cells that has been widely exploited for antimalarial drug discovery or mode-of-action studies^{17–21}. Yeast has an unparalleled toolset for genetics and synthetic biology, and is a valuable host for heterologous expression of functional *Plasmodium* spp. proteins^{22–24}. Previously, yeast genomic tools were used to reveal a novel mechanism of quinoline drug action, centred on cellular tryptophan (Trp) starvation. This action results from competition between drug and tryptophan for the high affinity yeast tryptophan/tyrosine transporter, Tat2p²⁰. Subsequently, the link between tryptophan and quinine action was successfully extended to malaria patients, where it was found that individuals with higher plasma tryptophan levels had a low incidence of adverse reactions to quinine²⁵. Furthermore, quinine perturbs biosynthesis and function of the major neurotransmitter serotonin, a metabolic product of tryptophan^{19,26}.

In the present work, the earlier findings with yeast are exploited to test function of a Tat2p structural homologue that we identify in *Plasmodium* spp. It transpires that this homologue is a putative amino acid transporter in which SNPs were previously linked to chloroquine resistance in malaria parasites^{27,28}. A recent attempt at characterisation by heterologous expression in *Xenopus laevis* oocytes did not produce detectably-functional protein²⁹. Here we successfully apply a yeast heterologous expression system to show that the parasite protein mediates uptake of quinoline drugs so altering the level of drug resistance. The evidence suggests a new quinoline–drug transport protein, which may help explain the protein's association with drug resistance of the parasite.

Results

The *P. falciparum* orthologue of *P. chabaudi aat1* and yeast *TAT2* mediates chloroquine uptake and toxicity.

The high affinity yeast tryptophan transporter Tat2p was previously found to transport quinine into cells, leading to quinine toxicity²⁰. Here, standard BLAST searches for homologues of yeast Tat2p among *Plasmodium* spp. revealed no hits. However, an HHPRED homology search against Tat2p based on predicted secondary structures (see Methods) identified the putative amino acid transporter PF3D7_0629500 from *P. falciparum* (PlasmoDB: PFF1430c, Uniprot ID:C6KTD0, E-value 1.8e-17, Probability 99.87; note that E-value < 1 and probability > 95 indicate statistically significant homology: https://toolkit.tuebingen.mpg.de/hhpred/help_ov#evalues) (Supplementary Fig. S1). PF3D7_0629500 was 82nd in a ranking of the proteins most-homologous to Tat2p among all available proteomes in HHPRED, and was the most significant homologue from *P. falciparum*. HHPred performs alignments of a protein amino acid sequence to secondary structure databases. No such database currently exists for certain species, such as the rodent parasite *P. chabaudi*, therefore we could not search Tat2p against all parasite species. However, PF3D7_0629500 is a known homologue of AAT1 from *P. chabaudi*, and a SNP in the *aat1* gene was previously linked with parasite resistance to chloroquine, a quinine derivative²⁷. SNPs in *PF3D7_0629500* have also been associated with chloroquine resistance in *P. falciparum*²⁸. Considering the evidence collectively, we hypothesized that the parasite protein may have a chloroquine and/or quinine transport function, resulting in toxicity if expressed heterologously in yeast. To test this, a codon optimised construct of the *PF3D7_0629500* ORF was cloned into the pCM190 expression vector. For heterologous expression of the parasite protein we capitalised on the availability of the yeast *trp1*Δ background. This strain is defective for tryptophan biosynthesis, similar to the parasite, and the strain's dependency on exogenous tryptophan gives more sensitive detection of sensitivity to quinoline antimalarials²⁰. Expression of PF3D7_0629500 in *trp1*Δ yeast conferred a chloroquine hypersensitivity phenotype (Fig. 1A). The cell doubling-time in the presence of CQ was 4-fold longer for cells expressing the parasite protein than empty vector control. In the absence of CQ, PF3D7_0629500 expression alone caused a small slowing of growth but the inhibitory effect attributable specifically to CQ remained considerably greater in these cells than in the empty vector control. To test whether the chloroquine sensitivity of PF3D7_0629500-expressing cells was related to increased chloroquine uptake, the chloroquine probe LynxTag-CQTM was used to measure cellular chloroquine accumulation with flow cytometry. Chloroquine accumulation plateaued from ~10 min. After 15 min, PF3D7_0629500-expressing cells had accumulated ~38% more drug than empty-vector control cells (p < 0.05, Student's t-test, one-tailed) (Fig. 1B). The results are consistent with the hypothesis that PF3D7_0629500 mediates elevated uptake of chloroquine, leading to drug hyper-sensitivity.

Complementation of yeast Tat2 and tryptophan-sensitivity of PF3D7_0629500 activity.

The *trp1*Δ background used above, necessary to detect Tat2-suppressible quinoline sensitivity in yeast, was not suitable for testing complementation of Tat2 function by PF3D7_0629500 because a *trp1*Δ/*tat2*Δ deletant is inviable^{20,30}. However, decreased uptake of quinine was previously demonstrated in the *tat2*Δ single-deletant^{20,30}. Therefore, we used this phenotype to test complementation of Tat2 function by PF3D7_0629500. We used an assay based on quinine absorbance at 350 nm³¹, which produced a linear relationship over a range of quinine concentrations relevant to our assay (Supplementary Fig. S2A) and which demonstrated time-dependent saturation of uptake by cells (Supplementary Fig. S2B). The *tat2*Δ deletion mutant accumulated ~75% less quinine than the wild type yeast (Fig. 2). This impairment of uptake was fully rescued by expression of the parasite protein (which also produced increased quinine uptake in the wild type yeast background). Previously, quinine sensitization mediated by the yeast tryptophan-permease Tat2 was shown to be suppressible by added tryptophan²⁰. Here,

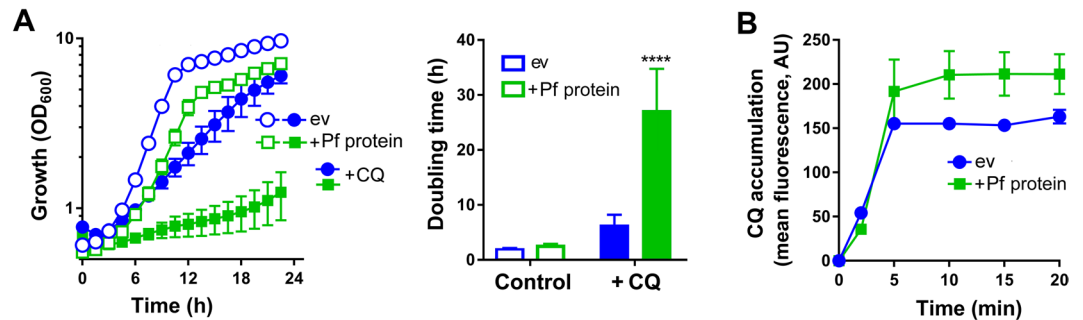


Figure 1. Expression of PF3D7_0629500 increases chloroquine uptake and toxicity. **(A)** Yeast *trp1*Δ cells transformed with pCM190 vector, either empty (ev) or containing the *PF3D7-0629500* ORF (Pf protein), were grown either with or without 1 mM chloroquine (CQ) (1 mM CQ was used in order to elicit yeast growth effects in the present assay system). Cell doubling times (right panel) were calculated from the exponential growth phase and the relevant treatments are as indicated on the panel. **(B)** Yeast *trp1*Δ cells transformed as in **(A)** were incubated in the presence of 0.4 mM chloroquine spiked with 20 μM LynxTag-CQ™. Cellular LynxTag-CQ™ was determined at intervals with flow cytometry, and cellular autofluorescence subtracted. AU, arbitrary units. All values are means ± SEM from three independent determinations. ****, $p < 0.0001$ according to multiple comparisons (with Tukey correction) by two way ANOVA.

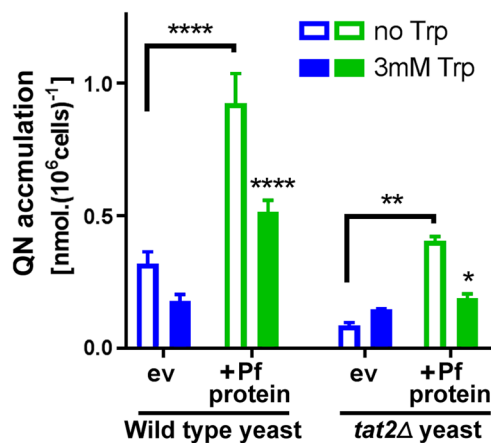


Figure 2. Complementations of yeast Tat2 and tryptophan-sensitivity of PF3D7_0629500 activity. Wild type or *tat2*Δ yeast cells transformed with pCM190 vector, either empty (ev) or containing the *PF3D7-0629500* ORF (Pf protein), were incubated for 20 min with 4 mM quinine either with or without 3 mM tryptophan (Trp). NaOH (6 mM) was included in all incubations to balance NaOH carry-over from tryptophan stock solution (NaOH had a small stimulatory effect on measured quinine uptake). Quinine analysis in cell lysates was according to absorbance determinations at 350 nm, normalised for cell numbers determined just before lysis, with subtraction of background (minus-quinine). * $p < 0.05$; ** $p < 0.01$; **** $p < 0.0001$; according to multiple comparisons (Sidak's test) by two way ANOVA.

inclusion of tryptophan (3 mM) significantly decreased PF3D7_0629500-dependent quinine uptake, measured in the *tat2*Δ background (Fig. 2). Therefore, PF3D7_0629500 could replace the tryptophan-suppressible quinine uptake activity of its yeast structural homologue.

Sensitization to several quinoline antimalarials is suppressible with the T162E SNP or tryptophan. We introduced a T162E mutation to PF3D7_0629500, which corresponded to the SNP previously linked to chloroquine resistance in *P. chabaudi*²⁷. Furthering that association described in the parasite, yeast cells expressing the mutant construct were considerably more resistant to chloroquine than cells expressing the wild-type parasite protein. That is, introduction of the T162E SNP rescued CQ hypersensitivity of PF3D7_0629500-expressing cells (Fig. 3A). The SNP also rescued the mildly-slowed growth of the PF3D7_0629500-expressing cells seen in the absence of drug. The SNP version of the parasite gene was expressed at least as strongly in yeast as the wild type version. This was shown by qRT-PCR (Fig. 3B), and by measurement of expressed protein levels with western blotting or flow cytometry (Supplementary Fig. S3). (There was also no discernible difference in localization of the two versions of the protein; see below).

We tested yeast expressing PF3D7_0629500 against several related drugs. As observed with chloroquine, PF3D7_0629500 expression conferred hypersensitivity to amodiaquine (weakest phenotype), mefloquine and quinine (strongest phenotype). This indicates that the parasite protein determines sensitivity to multiple

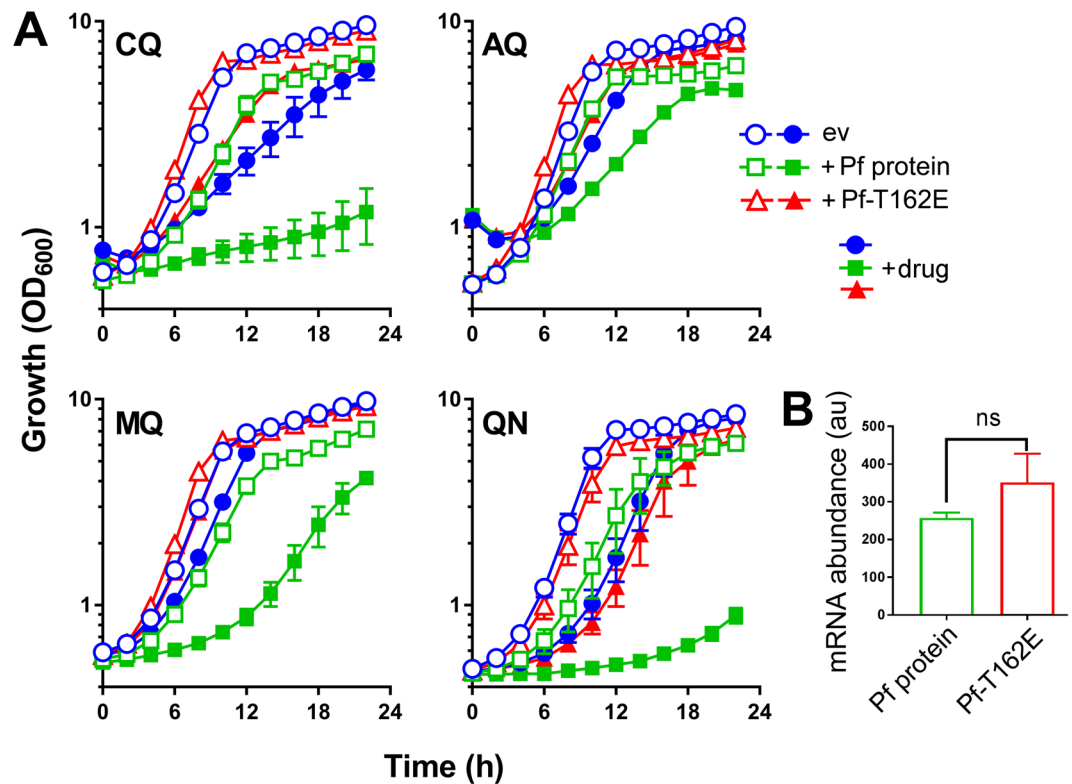


Figure 3. Sensitization to several quinoline antimalarials by PF3D7_0629500 expression and reversal with the T162E SNP. **(A)** Yeast *trp1*Δ cells transformed with pCM190 vector, either empty (ev) or expressing PF3D7_0629500 (Pf protein) or the same protein carrying the T162E SNP (Pf-T162E), were cultured with either 1 mM chloroquine (CQ), 1 mM amodiaquine (AQ), 25 μM mefloquine (MQ) or 3 mM quinine (QN). Mean data are shown from at least three independent experiments ± SEM. **(B)** RNA was extracted from wild type yeast transformed as in (A) and mRNA corresponding to the wild type *PF3D7-0629500* ORF or SNP (T162E) version was analysed with qRT-PCR, performed in triplicate for each condition. The same amount of RNA extract was used for each reaction. There was not a significant difference (ns, according to Student's *t*-test, two tailed) between the conditions either when compared by raw counts (as shown) or after normalization against *ACT1* mRNA. au, arbitrary units.

quinolines. In all cases, the SNP corresponding to that identified previously in the parasite reversed the sensitivity phenotypes (Fig. 3A). IC_{50} values were derived from growth rate data at varying doses of the drugs which gave the strongest phenotypes above. For cells expressing empty vector, PF3D7_0629500 or the SNP construct, respectively, IC_{50} values were 3.56, 2.92 or 3.42 mM for quinine and 0.694, 0.435 or 1.037 mM for chloroquine. (In the case of chloroquine, cells expressing the T162E SNP construct were even more resistant to drug than cells expressing empty vector.) Previously, as with quinine uptake (above), quinine sensitization mediated by the yeast Tat2 was shown to be suppressible by tryptophan²⁰. Here, inclusion of tryptophan in the medium also suppressed PF3D7_0629500-mediated sensitization to quinine (Fig. 4), further supporting a similar competition between drug and amino acid at this proposed transporter from the parasite.

Relationship between quinine uptake, quinine sensitivity and membrane-localization of PF3D7_0629500 in individual cells.

Quinine uptake was assayed in the *trp1*Δ yeast background (versus *tat2*Δ background in Fig. 2 above) so we could test whether quinine sensitization (Fig. 3A) was correlated with increased drug uptake in PF3D7_0629500-expressing cells, as was the case with chloroquine (Fig. 1). A rapid (≤ 30 s) initial association of quinine with cells (probably reflecting non-specific cell surface binding) was followed by continued accumulation of the drug in the PF3D7_0629500-expressing culture, but not in the empty vector control (Fig. 5A). After 60 min, cells expressing the parasite protein had accumulated ~4-fold more drug. This increased uptake was abrogated by introduction of the T162E SNP (Fig. 5B). The data were consistent with the suggestion that increased drug uptake in PF3D7_0629500-expressing cells causes their quinine sensitivity.

Yeast Tat2p is a plasma membrane-localized transport protein³². In *P. falciparum*, PF3D7_0629500 has been reported to localize to the digestive vacuole membrane, observed using a fluorescent reporter fusion construct, in keeping with its putative function as an amino acid transporter³³. To localize PF3D7_0629500 in yeast we expressed a GFP tagged version of the protein in the *tat2*Δ yeast background. Consistent with a transport function, the protein localized primarily to the yeast plasma membrane, co-localizing precisely with the membrane stain FM4-64 (a short FM4-64 staining time was used to restrict staining to the plasma membrane³⁴) (Fig. 6A). There was no apparent difference in localization of the PF3D7_0629500 protein versus the same protein carrying

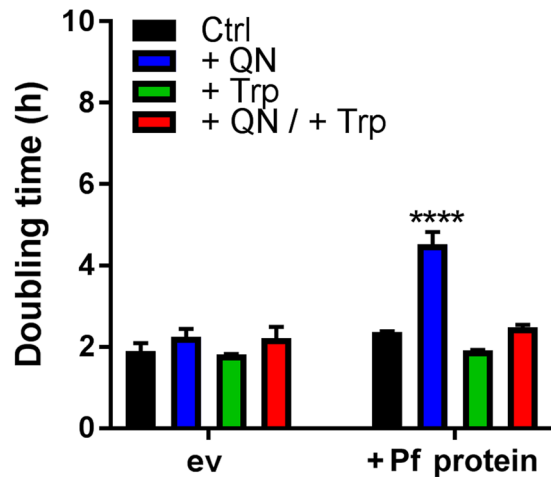


Figure 4. Sensitization to quinine in PF3D7_0629500-expressing cells is tryptophan suppressible. Yeast *trp1*Δ cells transformed with pCM190 vector, either empty (ev) or expressing PF3D7-0629500 (Pf protein), were cultured as specified either with or without 3 mM quinine and/or 1 mM tryptophan (Trp). Cell doubling times were calculated during the exponential phase of growth. Mean data are shown from at least three independent experiments ± SEM. **** $p < 0.0001$ according to multiple comparisons (with Tukey correction) by two way ANOVA.

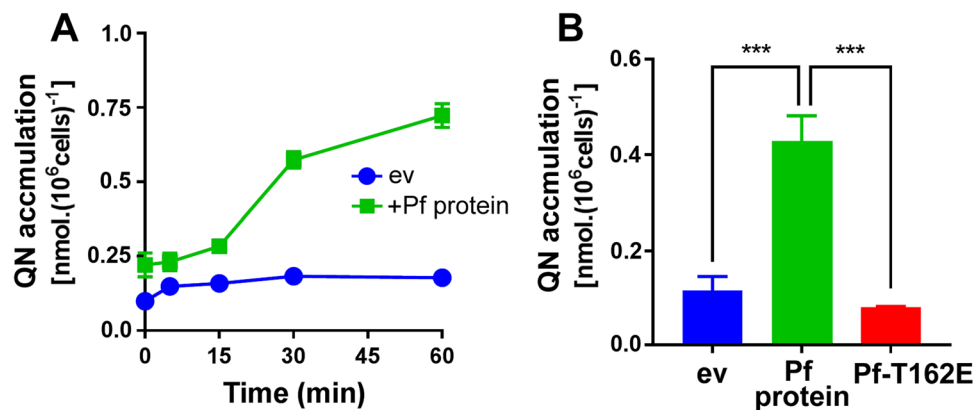


Figure 5. Increased quinine uptake in drug-sensitive PF3D7_0629500-expressing cells and reversal with the T162E SNP. (A) Yeast *trp1*Δ cells transformed with vector pCM190, either empty (ev) or expressing PF3D7-0629500 (Pf protein), were cultured with 4 mM quinine for the indicated time intervals before harvesting and lysis. Quinine analysis was as described in the Fig. 2 legend. (B) Yeast *trp1*Δ cells transformed with vector pCM190, either empty (ev), or expressing PF3D7-0629500 (Pf protein) or the same protein carrying the T162E SNP (Pf-T162E), were cultured for 20 min with 4 mM quinine before analysis of cellular quinine. Values are means ± SEM from three independent determinations. *** $p < 0.001$ according to multiple comparisons (with Tukey correction) by two way ANOVA.

the T162E SNP. The PfCRT transporter of the parasite's digestive-vacuole also localizes to the plasma membrane when expressed in yeast²⁴. Unexpectedly, there was visible heterogeneity between individual cells in their expression-level and localization of the protein: high-expressing cells are indicated by arrows, while comparison with the FM4-64 panels highlights certain cells that showed little or no PF3D7_0629500-associated GFP fluorescence (Fig. 6A). Heterogeneity of gene expression, protein localization or other phenotype between individual cells within genetically-uniform populations is described in other systems^{35–37}. Here, we exploited this phenomenon to interrogate further the relationship between PF3D7_0629500 expression-level and drug sensitivity. Again we exploited the *trp1*Δ background to help discern drug sensitivity. Heterogeneity in expression of PF3D7_0629500-GFP was quantifiable with flow cytometry, which indicated a broad non-normal distribution of cell fluorescences extending to almost two orders of magnitude greater than the mode cell-fluorescence (Fig. 6B). The > 100-fold total variation in expression level was comparable to that of one of the most variably expressed yeast proteins (a virulence factor of *Candida glabrata*) reported to date³⁸. Cell subpopulations were gated by their level of GFP fluorescence (Fig. 6B), then FACS sorted into four cell suspensions which were each assayed independently for quinine resistance. Quinine resistance was progressively eroded with increasing expression of PF3D7_0629500-GFP (Fig. 6C). The highest expressing fraction of cells showed no growth at 2 mM quinine.

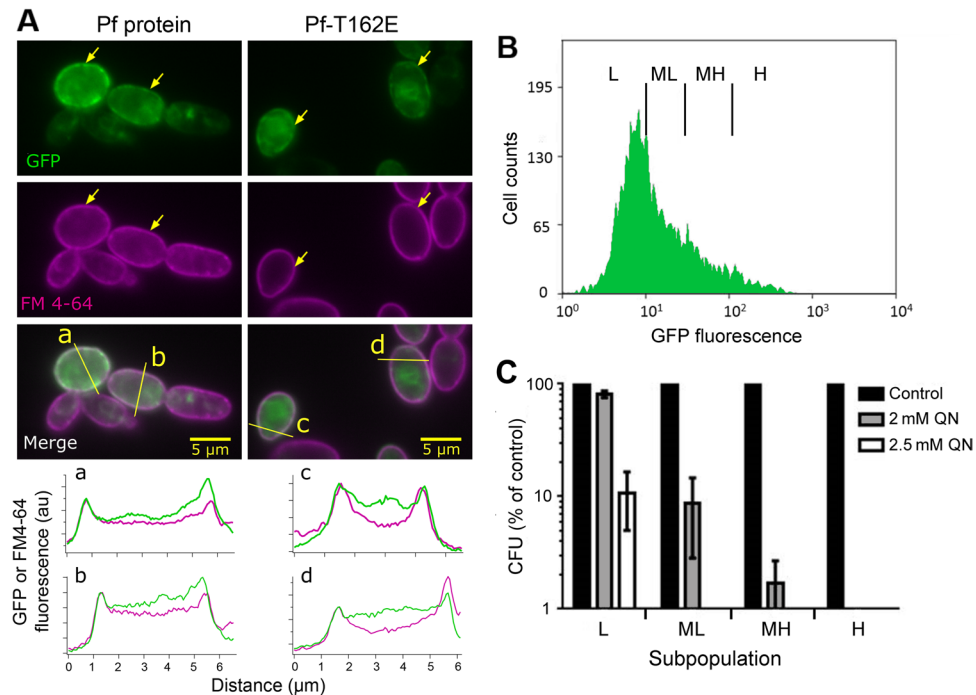


Figure 6. Heterogeneous expression of PF3D7_0629500 at the yeast plasma membrane determines individual-cell drug sensitivity. (A) Yeast *tat2*Δ cells expressing GFP-tagged PF3D7-0629500 (Pf protein) or Pf-T162E from vector pCM190 were stained with FM4-64 and examined by fluorescence microscopy. The fields of view shown are representative of several observed. Merged images (GFP in green, FM4-64 marker in magenta) are shown, as are the individual channels. Intensity line profiles along the lines (a, b, c, d) shown in the merged images are presented in the lower panels. Arrows indicate the high-expressing cells. au, arbitrary units. (B) Yeast *trp1*Δ cells expressing GFP-tagged PF3D7-0629500 were sorted into low (L), medium-low (ML), medium-high (MH) and high (H) -expressing cell subpopulations, according to GFP fluorescence; > 1,000 cells were sorted from each subpopulation. (C) Sorted cell subpopulations (B) were spread plated to YPD agar supplemented or not with quinine as indicated. Colony forming units (CFUs) were enumerated after 4 d incubation and expressed as a percentage of CFUs observed for the same cell subpopulation on minus-quinine control plates. Values are means ± SEM from three independent experiments.

In contrast, the lowest expressing cells retained > 80% outgrowth at 2 mM quinine, and ~10% outgrowth at 2.5 mM quinine. Results for medium expression-level populations supported this trend, albeit a little more variable between replicates. Therefore, reinforcing the observations with bulk cell populations (Fig. 3A), variation in single-cell expression level of PF3D7_0629500 affects the drug sensitivities of individual cells. Such variation itself can have important implications, as discussed further below.

Discussion

Previously it was found that, in yeast, quinine is specifically transported via the high-affinity aromatic amino acid transporter Tat2²⁰. The present study extrapolated this work to the *Plasmodium* parasite. The major finding from heterologous expression studies with PF3D7_0629500, a Tat2 structural-homologue identified from *P. falciparum*, was that the parasite protein determines quinine and chloroquine uptake and resistance when expressed in yeast. This homologue could not be identified using a standard BLAST search but was found with the HHPred tool which uses predicted secondary structures. Protein secondary structures diverge at a slower rate than amino acid sequence and so can help to identify more distant homologues^{39,40}.

The protein that is the focus of this work has previously been associated with quinoline resistance in the parasite. PF3D7_0629500 was identified by transcriptome profiling as one of only 45 genes differentially expressed between chloroquine-sensitive and -resistant mutants of *P. falciparum*⁴¹. Moreover, a non-synonymous SNP in AAT1 (the PF3D7_0629500 homologue of *P. chabaudi*) was a key determinant of chloroquine resistance in laboratory evolved parasites²⁷, and PF3D7_0629500 was recently associated with chloroquine resistance in *P. falciparum* by genome-wide association²⁸. However, the protein has not been subject to detailed study and its function is not previously established. Function could not be detected following heterologous expression in *Xenopus laevis* oocytes²⁹, in contrast to the yeast expression system described here. Reasons for this difference may include differences in protein folding or localization in the two expression systems. Reported vacuolar-membrane localization of the protein in the parasite translated into plasma membrane localization in yeast (see below), which was effective as the protein was functional. Yeast is well documented as a suitable host for heterologous expression of functional *Plasmodium* spp. proteins^{22–24}. The PF3D7_0629500 protein is expressed throughout the parasite intraerythrocytic cycle, at which most current antimalarials act^{42,43}, and is designated a putative amino acid transmembrane transporter based on sequence similarity. The protein has been reported to be expressed at the

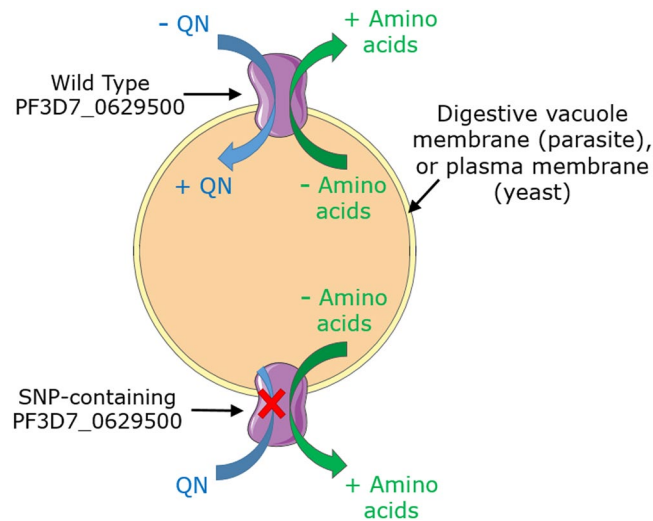


Figure 7. A model of PF3D7_0629500 action. PF3D7_0629500 is proposed to facilitate cross-membrane diffusion of amino acids or structurally-related quinolines down concentration gradients. In the parasite, this would probably enable release of amino acids from the digestive vacuole or entry of drug into the vacuole. In yeast, where the heterologous protein localizes to the plasma membrane, PF3D7_0629500 enables drug uptake into cells. The T162E SNP abrogates the drug transport function, decreasing drug accumulation at the respective sites of action in both organisms.

parasite's digestive vacuole membrane³³. Heterologous expression of the GFP tagged version in yeast gave localization primarily to the plasma membrane, providing a convenient system for assaying transport function via analysis of whole-cell drug contents after simple cell separation from medium.

The localization information helps rationalise the effects of the protein on drug resistance. In the parasite, PF3D7_0629500 is likely to mediate transport of a wide range of amino acids or small peptides from the parasite's digestive vacuole, where haemoglobin is digested^{42,44}. Such movement down the concentration gradient from vacuole to cytoplasm is consistent with a facilitated diffusion transport mechanism, as occurs in the yeast homologue Tat2. This is further supported by suggestions that PF3D7_0629500-mediated drug transport is passive, unaffected by incubation at 4 C or treatment with the protonophore CCCP (S. Tindall and S.V. Avery, unpublished data). It follows that, according to its localization, PF3D7_0629500 would facilitate transport of drug (down the concentration gradient) either from cytoplasm to vacuole in the parasite, or from extra- to intra-cellular in yeast (Fig. 7). In both cases, this represents transport of drug to its anticipated site of action (different in yeast and parasite) and is in keeping with the drug-sensitivity or -resistance phenotypes seen, respectively, with expression of the wild type or SNP (loss of drug transport) versions of the protein in yeast (present data) and parasite²⁷. The SNP introduced here corresponded to that found in the parasite-resistance study and which, we showed, impairs drug-transport function. The T162E SNP creates a more negative charge in a conserved region near the start of a transmembrane helix; a very similar effect to that of the K76T SNP in PfCRT which confers CQ resistance²⁷, discussed further below.

As with the yeast Tat2p transporter²⁰, PF3D7_0629500-dependent quinine sensitivity was suppressible with tryptophan. This suggests that as in yeast, the drug competes for uptake with tryptophan, a proposed natural substrate of the parasite protein. Such competition may be less relevant where drug and amino acid are moving down concentration gradients in opposite directions. Nonetheless, where it does occur, competition can be ascribed to the structural similarity of tryptophan and quinine, a drug that is derived enzymatically from tryptophan⁴⁵. Competition between quinine and tryptophan also raises the possibility that quinine displaces the essential amino acid intracellularly, e.g. during metabolism or protein synthesis²⁰. Tryptophan depletion arising in this way has been proposed to account for certain of the drug's adverse effects in quinine-treated malaria patients²⁵. It cannot be discounted that a similar tryptophan-depletion mechanism could contribute to quinine action in the parasite.

There was heterogeneity between cells in the level of GFP tagged PF3D7_0629500 expression in yeast. Such heterogeneity underscores how population averaged measurements can misrepresent the activities relevant to any individual cell⁴⁶. Phenotypic heterogeneity within genetically-uniform cell populations is thought to be a universal phenomenon, which has received increased scrutiny in recent years with the growing awareness of its potential role in the persistence of microbial infections and tumours^{38,47,48}. Typically, phenotypic heterogeneity within a clonal cell population is caused by gene-expression variation, arising from noise during transcription or translation, or cell cycle-, age-, or epigenetically-driven changes in expression. Epigenetic changes in the expression of surface antigens of *P. falciparum* are reported to help avoid host immune responses³⁵. The marked heterogeneity of PF3D7_0629500 expression seen in this study was exploited as a novel tool to dissect the relationship between drug sensitivity and PF3D7_0629500 expression, at an individual cell level. We cannot infer whether PF3D7_0629500 expression or membrane-localization is as heterogeneous in the parasite as is apparent in yeast. However, given the protein's evident function in quinoline-drug transport and toxicity, any heterogeneity could have important implications for malaria treatment with quinolines. In bacteria, phenotypic heterogeneity is well known to create phenotypically resistant sub-populations – persister cells – which may re-initiate infection when antimicrobial

therapy is stopped⁴⁸. To date there has been less work of a similar nature in *Plasmodium* spp., although “dormancy” in the parasite could have a similar effect as antimicrobial persistence⁴⁹. The present results suggest a possibility that PF3D7_0629500 might be a good candidate for further study. Moreover, gene expression heterogeneity within clonal *Plasmodium* spp. populations could be an important gap in current drug resistance models.

Several parallels have previously been noted between PF3D7_0629500 and PfCRT, the best studied chloroquine resistance determinant in *P. falciparum*. Both are thought to serve as channel proteins on the digestive vacuole membrane, each containing 10 transmembrane domains^{27,50}. Both may be involved in the transport of amino acids or small peptides^{42,51}. Furthermore, inhibition of PfCRT-mediated amino acid and peptide transport by chloroquine has been suggested potentially to contribute to the drug’s inhibitory action⁵¹. A similar potential action is discussed above for PF3D7_0629500. Finally, mutations in PfCRT have been shown to alter sensitivity to further quinolines, such as quinine, amodiaquine and mefloquine^{52,53}. PF3D7_0629500 expression sensitized yeast to all the quinoline antimalarials that were tested in this study. The evidence suggests that PF3D7_0629500 could be important as a multi-drug sensitivity/resistance determinant in *Plasmodium* spp.

The weight of published evidence remains with PfCRT (in particular the K76T SNP) as the foremost marker of chloroquine resistance in isolates of *P. falciparum*. A similar strong marker has not been found with the *P. vivax* homologue (PvCRT)^{54,55}, although there is evidence that chloroquine resistance may be conferred by changes in levels of PvCRT (or PvMDR1) expression⁵⁶. It would be of interest to investigate the *P. vivax* orthologue of PF3D7_0629500 (PVP01_1120000) as a potential resistance marker in *P. vivax*, where resistance to chloroquine is a growing concern⁵⁷.

Among the current malaria treatment options, quinolines are commonly combined with artemisinin (or artemisinin derivative) in antimalarial combination treatments (ACTs). Therefore, it is worth noting that a SNP in PF3D7_0629500 (S258L) has previously been associated with artemisinin-resistant subpopulations of clinical *P. falciparum* isolates⁷. Any evolutionary selection of this SNP is not necessarily artemisinin-driven, as mutations conferring artemisinin resistance can be selected before a population has been exposed to the drug⁵⁸. Moreover, given the present data and considering the prevalence of ACT therapy, we also suggest the possibility that selection for the S258L SNP could have been driven by quinolines used in combination with artemisinin.

In conclusion, rationalising previous observations with malaria parasites, the heterologous expression studies presented here reveal that PF3D7_0629500 activity can determine the transport and action of multiple quinoline drugs. Furthermore, cell-cell heterogeneity in PF3D7_0629500 activity provided a novel tool to corroborate that relationship, while suggesting the tantalising possibility of heterogeneous activity also in the parasite and attendant implications for modelling quinoline drug resistance. Finally, the results reinforce the value of model systems for uncovering or substantiating novel protein functions that may have an important bearing on the spread (and control) of antimalarial drug resistance.

Methods

Bioinformatic analysis. The online tool HHPRED⁴⁰ (available at <http://toolkit.tuebingen.mpg.de/hhpred>) was used to find orthologues of the *S. cerevisiae* high-affinity tryptophan transporter, Tat2, in *P. falciparum*. The Tat2 amino acid sequence from *S. cerevisiae* (UniProt P38967) was used as a query sequence in HHPRED using the *Plasmodium falciparum* and *Saccharomyces cerevisiae* databases as the target proteomes. All other options were at default settings. This seed query generated a multiple alignment of homologues using multiple iterations of PSI-BLAST. A secondary structure prediction was carried out and annotated on the final alignment using PSIPRED⁵⁹ from which a profile Hidden Markov Model (HMM) is derived. HMM-to-HMM comparisons were carried out against all available HMM databases in the target proteomes to locate homologues based on similarity of predicted secondary structure rather than sequence alone.

Yeast strains and culture conditions. The *S. cerevisiae* diploid strain BY4743 (*MATa/MAT α his3-1/his3-1 leu2-0/leu2-0 met15-0/MET15 LYS2/lys2-0 ura3-0/ura3-0*), and isogenic deletion mutants *trp1*Δ and *tat2*Δ were from Euroscarf (Frankfurt, Germany). Yeast were maintained and grown in YPD medium (2% peptone, 1% yeast extract, 2% D-glucose; Oxoid, Basingstoke, UK), or YNB medium (0.69% yeast nitrogen base without amino acids; Formedium; Norfolk, UK) supplemented with 2% (*w/v*) D-glucose and as appropriate for plasmid selection⁶⁰. Where necessary, media were solidified with 2% (*w/v*) agar (Sigma). To culture organisms for experiments, single colonies were used to inoculate broth cultures in Erlenmeyer flasks and incubated at 30 °C with orbital shaking at 120 rev min⁻¹. The same procedure was used for all strains.

Growth inhibition assays. For continuous growth assays with the different yeast strains, mid/late-exponential cultures were diluted to OD₆₀₀~0.1 and 300 μl aliquots transferred to 48-well microtiter plates (Greiner Bio-One; Stonehouse, UK) with antimalarial drugs added as specified and balanced for any solvent additions. Plates were incubated at 30 °C with shaking in a BioTek Powerwave XS microplate spectrophotometer and OD₆₀₀ was recorded every 30 min. Cell doubling times were calculated from the linear portion of exponential growth. Drug concentrations giving 50% growth inhibition (IC₅₀ values) were determined from doubling-time data at different drug concentrations. Antimalarial drugs used were amodiaquine dihydrochloride dihydrate (AMQ), chloroquine diphosphate salt (CQ), mefloquine hydrochloride (MQ) and quinine dihydrochloride (QN) (Sigma). Drugs were dissolved in water except quinine and mefloquine which were prepared in 70% (*v/v*) ethanol stock solutions, diluted to 0.5% final ethanol concentration for experiments. Ethanol at 0.5% has no effect on yeast viability and was balanced in relevant control incubations. Tryptophan additions were from stock solutions of 0.5 M L-tryptophan (Sigma) prepared in 1 M NaOH. NaOH (6 mM) was included in relevant control incubations to balance NaOH carry-over from the tryptophan stock solution. For assays based on colony forming ability, FACS-sorted cell subpopulations (see below) were diluted in PBS to OD₆₀₀~5 × 10⁻⁵ (~1500 cells ml⁻¹) and 200 μl aliquots spread-plated to YPD agar plates supplemented with QN as specified. Colony forming units (CFUs) were counted after 4 d incubation at 30 °C.

Heterologous expression of PF3D7_0629500 and Introduction of SNPs. A yeast-codon optimised *PF3D7_0629500* gene cloned in the pUC57 vector was a kind gift from Enrique Salcedo-Sora (Liverpool Hope University). For expression in yeast, *NotI* and *PmeI* sites were added to the 5' and 3' termini of the *PF3D7_0629500* ORF by PCR and the product ligated between these restriction sites in the pCM190 vector⁶¹. This placed the ORF under the control of the doxycycline-regulatable *tetO* promoter. To introduce a T162E SNP into *PF3D7_0629500*, the Q5 site-directed mutagenesis kit was used according to the manufacturer's instructions [New England Biolabs (NEB); Hitchin, UK]. Introduction of the SNP was verified by sequencing. Recombinant plasmids were transformed into *S. cerevisiae* using the lithium acetate method⁶². To tag *PF3D7_0629500* and *PF3D7_0629500*^{T162E} with GFP, *BstBI* and *AscI* sites were added to the 5' and 3' termini of the relevant ORF by PCR and the product ligated between these restriction sites in the pFA6a-GFP(S65T)-His3MX6 vector⁶³. The EGFP cassette with a fragment of the *PF3D7_0629500* or *PF3D7_0629500*^{T162E} ORF up to its 3' *BlpI* digestion site was then PCR amplified with the addition of a 5' *SfiI* site and ligated in frame to pCM190-*PF3D7_0629500*. Primer sequences are available on request. Transformed yeast were grown on YNB medium with appropriate supplements for selection. All DNA cloning and genetic manipulations were performed in *Escherichia coli* XL1-blue cells. PCR, restriction digests and ligations were carried out using standard protocols⁶⁴.

RNA extraction and quantitative RT-PCR (qRT-PCR). mRNA from specified genes in plasmid-transformed *S. cerevisiae* BY4743 was quantified by qRT-PCR exactly as described previously⁶⁵, except that RNA was isolated by the "hot phenol" technique then treated with Amplification Grade DNase I (Sigma-Aldrich, St. Louis, MO), and 25 ng cDNA with 175 nM gene-specific primers (sequences available on request) were used in the PCR reactions. PCRs were carried out for 40 cycles; denaturation at 95 °C for 15 s, annealing/extension at 60 °C for 30 s. Melting-curve analysis confirmed a single PCR product. Amplification was quantified from a standard curve constructed from reactions with defined genomic DNA concentrations.

Fluorescence microscopy and FACS. For examination of GFP fluorescence by microscopy and flow cytometry, exponential-phase yeast cells were washed with PBS, and imaged with a DeltaVision Elite microscope (GE Healthcare Life Sciences, UK) equipped with a Photometrics CoolSnap HQ2 camera (Photometrics, USA), or analysed with a Beckman Coulter FC500 cytometer. Staining for ~5 min with FM4-64 (SynaptoRed reagent; Calbiochem, EMD Biosciences, San Diego, CA) was performed as described previously³⁴. Microscopic images were acquired with a 100 × 1.4 NA objective lens. GFP fluorescence was captured using the FITC filter set, and FM4-64 using the TRITC filter for excitation and the Cy-5 filter for emission; the Quad polychroic was used for both channels. Exposure times were the same for the different strains; 0.4 s and 0.05 s for the FITC and Cy-5 channels, respectively. Images were collected in a single z-plane. Images, line profiles and landmarks were produced in Fiji (<https://imagej.net/Fiji>) and Igor Pro (Wavemetrics, USA) and images assembled in Inkscape (<http://www.inkscape.org/>). To FACS-sort cells, yeast expressing *PF3D7_0629500*-GFP were harvested by centrifugation (3,220 g, 3 min) and resuspended in PBS at OD₆₀₀ ~ 2.0, before gating and sorting with a Beckman Coulter MoFlo XDP flow cytometer, equipped with a 488 nm laser. Emitted GFP fluorescence was collected using a 529/28 nm band pass filter. FACS-sorted cell subpopulations were diluted in PBS and spread to YPD agar as described above.

Preparation of protein extracts and western blotting. Cells were collected by centrifugation, washed serially with cold water and lysis buffer (50 mM Tri-HCl, 500 mM NaCl, pH 7.4, supplemented with protease inhibitors: 1 mM PMSE, 4 mM benzamidine hydrochloride, 2.5 mM EDTA, pH 8) then disrupted with glass beads⁶⁶. Lysates were treated with 1% Triton X-100 on ice for 30 min and then with cracking buffer (8 M Urea, 5% (w/v) SDS, 40 mM Tris-HCl pH 6.8, 0.1 mM EDTA, 0.4 mg/ml bromophenol blue) at 37 °C for 10 min followed by incubation at 95 °C for a further 10 min. For western blotting, proteins were separated by electrophoresis on 10% (w/v) NuPAGE Bis-Tris gels (Life Technologies) before transfer to nitrocellulose membrane (GE Healthcare). Protein loading was shown by staining with Ponceau S (Sigma). Immunodetection of GFP tagged proteins was with anti-GFP primary antibody (1:1000 dilution; Roche) and poly horseradish peroxidase (poly HRP) conjugated goat anti-mouse antibody (1:10000 dilution; Thermo Scientific). GFP tagged proteins were detected with an electrochemiluminescence HRP kit (Pierce) and imaged using a Chemidoc XRS (Bio-Rad). Protein band intensities were quantified with ImageJ software.

Assays of drug uptake. Quinine uptake was assayed essentially as described previously⁶⁷, except that quinine absorbance at 350 nm³¹ was measured instead of quinine fluorescence. Briefly, overnight cultures were diluted to OD₆₀₀ 0.1 in fresh YPD medium and cultured for a further 4 h with shaking. Quinine was added to a final concentration of 4 mM and cells incubated at 30 °C, 120 rev min⁻¹. At intervals, cells were harvested by centrifugation (3,220 g, 3 min), washed three times with ice cold water and resuspended in 10% (w/v) perchloric acid, 2 M sodium methanesulfonate together with an equal volume of acid-washed glass beads (425–600 μm, Sigma). Cells (~3.7 × 10⁸ in 800 μl) were lysed by 3 × 1-min vortexing with beads interspersed with 1 min incubations on ice, centrifuged at 16,060 g, 5 min, before 20 μl supernatant (corresponding to lysate from ~1 × 10⁷ cells) was diluted with 180 μl lysis buffer and A₃₅₀ measured with an Ultrospec 2000 UV/visible spectrophotometer (Amersham Pharmacia Biotech; Amersham, UK). Values for A₃₅₀ were normalised against OD₆₀₀ determinations taken just before cell lysis. (The OD₆₀₀ determinations provided estimates of the cell concentrations.) Chloroquine uptake by cells was estimated using a fluorescently-labelled chloroquine molecule, LynxTag-CQTM Green (BioLynx Technologies), as described previously⁶⁸. Fluorescence from cellular LynxTag-CQTM Green was measured with a Beckman Coulter FC500 flow cytometer, with excitation at 488 nm. Cell autofluorescence was subtracted.

Data availability. No large datasets were generated or analysed during the current study. Other data are available from the author on reasonable request.

References

- Cowman, A. F., Healer, J., Marapana, D. & Marsh, K. Malaria: Biology and disease. *Cell* **167**, 610–624 (2016).
- WHO. Fact Sheet: World Malaria Report 2015. Retrieved 23 November 2016 (2015).
- Achan, J. *et al.* Quinine, an old anti-malarial drug in a modern world: role in the treatment of malaria. *Malaria J.* **10**, 144 (2011).
- Hill, J. *et al.* Women's access and provider practices for the case management of malaria during pregnancy: a systematic review and meta-analysis. *PLoS Med.* **11**, e1001688 (2014).
- WHO. *Guidelines for the Treatment of Malaria - third edition* (2015).
- Henriques, G. *et al.* The mu-subunit of *Plasmodium falciparum* clathrin-associated adaptor protein 2 modulates *in vitro* parasite response to artemisinin and quinine. *Antimicrob. Ag. Chemother.* **59**, 2540–2547 (2015).
- Miotto, O. *et al.* Multiple populations of artemisinin-resistant *Plasmodium falciparum* in Cambodia. *Nat. Genet.* **45**, 648–655 (2013).
- Chang, G. Multidrug resistance ABC transporters. *FEBS Lett.* **555**, 102–105 (2003).
- Kell, D. B. & Oliver, S. G. How drugs get into cells: tested and testable predictions to help discriminate between transporter-mediated uptake and lipoidal bilayer diffusion. *Front. Pharmacol.* **5**, 231 (2014).
- Petersen, I., Eastman, R. & Lanzer, M. Drug-resistant malaria: Molecular mechanisms and implications for public health. *FEBS Lett.* **585**, 1551–1562 (2011).
- Ecker, A., Lehane, A. M., Clain, J. & Fidock, D. A. PfCRT and its role in antimalarial drug resistance. *Trends Parasitol.* **28**, 504–514 (2012).
- Huang, B. *et al.* Prevalence of *crt* and *mdr-1* mutations in *Plasmodium falciparum* isolates from Grande Comore island after withdrawal of chloroquine. *Malaria J.* **15**, 414 (2016).
- Mwai, L. *et al.* Chloroquine resistance before and after its withdrawal in Kenya. *Malaria J.* **8**, 106 (2009).
- Fairhurst, R. M. & Dondorp, A. M. Artemisinin-resistant *Plasmodium falciparum* malaria. *Microbiol. Spectr.* **4**, EI10-0013–2016 (2016).
- Ganesan, S. M., Falla, A., Goldfless, S. J., Nasamu, A. S. & Niles, J. C. Synthetic RNA-protein modules integrated with native translation mechanisms to control gene expression in malaria parasites. *Nature Comm.* **7**, 10727 (2016).
- Ghorbal, M. *et al.* Genome editing in the human malaria parasite *Plasmodium falciparum* using the CRISPR-Cas9 system. *Nature Biotech.* **32**, 819–821 (2014).
- Balana-Fouce, R. & Reguera, R. M. Yeast-based systems for tropical disease drug discovery. *Expert Op. Drug Discov.* **11**, 429–432 (2016).
- dos Santos, S. C. & Sa-Correia, I. A genome-wide screen identifies yeast genes required for protection against or enhanced cytotoxicity of the antimalarial drug quinine. *Mol. Genet. Genom.* **286**, 333–346 (2011).
- Islahudin, F. *et al.* The antimalarial drug quinine interferes with serotonin biosynthesis and action. *Sci. Rep.* **4**, 3618 (2014).
- Khozoie, C., Pleass, R. J. & Avery, S. V. The antimalarial drug quinine disrupts Tat2p-mediated tryptophan transport and causes tryptophan starvation. *J. Biol. Chem.* **284**, 17968–17974 (2009).
- Li, W. *et al.* Yeast model uncovers dual roles of mitochondria in the action of artemisinin. *PLoS Genet.* **1**, e36 (2005).
- Bilsland, E. *et al.* Functional expression of parasite drug targets and their human orthologs in yeast. *PLoS Negl. Trop. Dis.* **5**, e1320 (2011).
- Slavic, K. *et al.* A vacuolar iron-transporter homologue acts as a detoxifier in *Plasmodium*. *Nat. Comm.* **7**, 10403 (2016).
- Zhang, H. B., Howard, E. M. & Roepe, P. D. Analysis of the antimalarial drug resistance protein PfCRT expressed in yeast. *J. Biol. Chem.* **277**, 49767–49775 (2002).
- Islahudin, F., Pleass, R. J., Avery, S. V. & Ting, K.-N. Quinine interactions with tryptophan and tyrosine in malaria patients, and implications for quinine responses in the clinical setting. *J. Antimicrob. Chemother.* **67**, 2501–2504 (2012).
- Thompson, A. J. & Lummis, S. C. R. Antimalarial drugs inhibit human 5-HT₃ and GABA_A but not GABA_C receptors. *Brit. J. Pharmacol.* **153**, 1686–1696 (2008).
- Modrzynska, K. K. *et al.* Quantitative genome re-sequencing defines multiple mutations conferring chloroquine resistance in rodent malaria. *BMC Genom.* **13**, 106 (2012).
- Wang, Z. L. *et al.* Genome-wide association analysis identifies genetic loci associated with resistance to multiple antimalarials in *Plasmodium falciparum* from China-Myanmar border. *Sci. Rep.* **6**, 33891 (2016).
- Cobbold, S. A., Llinas, M. & Kirk, K. Sequestration and metabolism of host cell arginine by the intraerythrocytic malaria parasite *Plasmodium falciparum*. *Cellul. Microbiol.* **18**, 820–830 (2016).
- Khozoie, C., Pleass, R. J. & Avery, S. V. The antimalarial drug quinine disrupts Tat2p-mediated tryptophan transport and causes tryptophan starvation. *J. Biol. Chem.* **284**, 17968–17974 (2009).
- Lakowicz, J. R. *Principles of Fluorescence Spectroscopy*. 3 edn. (Springer-Verlag, 2006).
- Umebayashi, K. & Nakano, A. Ergosterol is required for targeting of tryptophan permease to the yeast plasma membrane. *J. Cell Biol.* **161**, 1117–1131 (2003).
- Moura, P. A. *Novel insights into the digestive vacuole biology of the malarial parasite Plasmodium falciparum*. PhD thesis, Yeshiva University, (2008).
- Holland, S. L. & Avery, S. V. Actin-mediated endocytosis limits intracellular Cr accumulation and Cr toxicity during chromate stress. *Toxicol. Sci.* **111**, 437–446 (2009).
- Guizetti, J. & Scherf, A. Silence, activate, poise and switch! Mechanisms of antigenic variation in *Plasmodium falciparum*. *Cellul. Microbiol.* **15**, 718–726 (2013).
- Hewitt, S. K., Foster, D. S., Dyer, P. S. & Avery, S. V. Phenotypic heterogeneity in fungi: Importance and methodology. *Fung. Biol. Rev.* **30**, 176–184 (2016).
- Symmons, O. & Raj, A. What's luck got to do with it: single cells, multiple fates, and biological nondeterminism. *Mol. Cell* **62**, 788–802 (2016).
- Halliwell, S. C., Smith, M. C. A., Muston, P., Holland, S. L. & Avery, S. V. Heterogeneous expression of the virulence-related adhesin Epa1 between individual cells and strains of the pathogen *Candida glabrata*. *Euk. Cell* **11**, 141–150 (2012).
- Siltberg-Liberles, J., Grahnen, J. A. & Liberles, D. A. The evolution of protein structures and structural ensembles under functional constraint. *Genes* **2**, 748–762 (2011).
- Soding, J., Biegert, A. & Lupas, A. N. The HHpred interactive server for protein homology detection and structure prediction. *Nucl. Acids Res.* **33**, W244–W248 (2005).
- Jiang, H. Y. *et al.* Genome-wide compensatory changes accompany drug-selected mutations in the *Plasmodium falciparum crt* gene. *PLoS One* **3**, e2484 (2008).
- Martin, R. E., Henry, R. I., Abbey, J. L., Clements, J. D. & Kirk, K. The 'permeome' of the malaria parasite: an overview of the membrane transport proteins of *Plasmodium falciparum*. *Genome Biol.* **6**, R26 (2005).
- Wilson, D. W., Langer, C., Goodman, C. D., McFadden, G. I. & Beeson, J. G. Defining the timing of action of antimalarial drugs against *Plasmodium falciparum*. *Antimicrob. Ag. Chemother.* **57**, 1455–1467 (2013).
- Kolakovich, K. A., Gluzman, I. Y., Duffin, K. L. & Goldberg, D. E. Generation of hemoglobin peptides in the acidic digestive vacuole of *Plasmodium falciparum* implicates peptide transport in amino acid production. *Mol. Biochem. Parasitol.* **87**, 123–135 (1997).

45. O'Connor, S. E. & Maresh, J. J. Chemistry and biology of monoterpene indole alkaloid biosynthesis. *Natural Product Rep.* **23**, 532–547 (2006).
46. Avery, S. V. Microbial cell individuality and the underlying sources of heterogeneity. *Nat. Rev. Microbiol.* **4**, 577–587 (2006).
47. Brock, A., Chang, H. & Huang, S. Non-genetic heterogeneity - a mutation-independent driving force for the somatic evolution of tumours. *Nature Rev. Genet.* **10**, 336–342 (2009).
48. Wood, T. K. Combatting bacterial persister cells. *Biotechnol. Bioeng.* **113**, 476–483 (2016).
49. Codd, A., Teuscher, F., Kyle, D. E., Cheng, Q. & Gatton, M. L. Artemisinin-induced parasite dormancy: a plausible mechanism for treatment failure. *Malaria J.* **10**, 56 (2011).
50. Fidock, D. A. *et al.* Mutations in the *P. falciparum* digestive vacuole transmembrane protein PfCRT and evidence for their role in chloroquine resistance. *Mol. Cell* **6**, 861–871 (2000).
51. Juge, N. *et al.* *Plasmodium falciparum* chloroquine resistance transporter is a H⁺-coupled polyspecific nutrient and drug exporter. *Proc. Natl. Acad. Sci. USA* **112**, 3356–3361 (2015).
52. Cooper, R. A. *et al.* Mutations in transmembrane domains 1, 4 and 9 of the *Plasmodium falciparum* chloroquine resistance transporter alter susceptibility to chloroquine, quinine and quinidine. *Mol. Microbiol.* **63**, 270–282 (2007).
53. Richards, S. N. *et al.* Molecular mechanisms for drug hypersensitivity induced by the malaria parasite's chloroquine resistance transporter. *PLoS Pathog.* **12**, e1005725 (2016).
54. Golassa, L., Erko, B., Baliraine, F. N., Aseffa, A. & Swedberg, G. Polymorphisms in chloroquine resistance-associated genes in *Plasmodium vivax* in Ethiopia. *Malaria J.* **14**, 164 (2015).
55. Nomura, T. *et al.* Evidence for different mechanisms of chloroquine resistance in 2 *Plasmodium* species that cause human malaria. *J. Infect. Dis.* **183**, 1653–1661 (2001).
56. Melo, G. C. *et al.* Expression levels of *pvcr-t* and *pvm-dr-1* are associated with chloroquine resistance and severe *Plasmodium vivax* malaria in patients of the Brazilian Amazon. *PLoS One* **9**, e105922 (2014).
57. Popovici, J. & Menard, D. Challenges in antimalarial drug treatment for vivax malaria control. *Trends Mol. Med.* **21**, 776–788 (2015).
58. Hunt, P. *et al.* Experimental evolution, genetic analysis and genome re-sequencing reveal the mutation conferring artemisinin resistance in an isogenic lineage of malaria parasites. *BMC Genom.* **11**, 499 (2010).
59. Jones, D. T. Protein secondary structure prediction based on position-specific scoring matrices. *J. Mol. Biol.* **292**, 195–202 (1999).
60. Moreno-Martinez, E., Vallieres, C., Holland, S. L. & Avery, S. V. Novel, synergistic antifungal combinations that target translation fidelity. *Sci. Rep.* **5**, 16700 (2015).
61. Gari, E., Piedrafitra, L., Aldea, M. & Herrero, E. A set of vectors with a tetracycline-regulatable promoter system for modulated gene expression in *Saccharomyces cerevisiae*. *Yeast* **13**, 837–848 (1997).
62. Gietz, R. D. & Woods, R. A. Transformation of yeast by lithium acetate/single-stranded carrier DNA/polyethylene glycol method. *Methods Enzymol.* **350**, 87–96 (2002).
63. Longtine, M. S. *et al.* Additional modules for versatile and economical PCR-based gene deletion and modification in *Saccharomyces cerevisiae*. *Yeast* **14**, 953–961 (1998).
64. Ausubel, F. M. *et al.* *Current Protocols in Molecular Biology*. (John Wiley & Sons, 2007).
65. Halliwell, S. C., Smith, M. C., Muston, P., Holland, S. L. & Avery, S. V. Heterogeneous expression of the virulence-related adhesin Epa1 between individual cells and strains of the pathogen *Candida glabrata*. *Eukaryot. Cell* **11**, 141–150 (2012).
66. Vallieres, C., Holland, S. L. & Avery, S. V. Mitochondrial ferredoxin determines vulnerability of cells to copper excess. *Cell Chem. Biol.* **24**, 1228–1237 (2017).
67. dos Santos, S. C., Tenreiro, S., Palma, M., Becker, J. & Sa-Correia, I. Transcriptomic profiling of the *Saccharomyces cerevisiae* response to quinine reveals a glucose limitation response attributable to drug-induced inhibition of glucose uptake. *Antimicrob. Ag. Chemother.* **53**, 5213–5223 (2009).
68. Islahudin, F. *et al.* Cell wall perturbation sensitizes fungi to the antimalarial drug chloroquine. *Antimicrob. Ag. Chemother.* **57**, 3889–3896 (2013).

Acknowledgements

This work was supported by the Biotechnology and Biological Sciences Research Council (BB/I000852/1 and BB/M022161/1). We thank Richard Pleass, Rita Tewari, Giancarlo Biagini and David Fidock for helpful discussions and Matt Kokolski for expert technical support. Imaging support was provided by the School of Life Sciences Imaging Unit supported by a Wellcome Trust Equipment Grant (094233/Z/10/Z).

Author Contributions

S.V.A. devised the study. S.M.T. and C.V. performed the experiments. S.M.T., C.V., D.H.L., F.I., K.N.T. and S.V.A. all contributed to experimental design and data interpretation. S.M.T. drafted the manuscript with input from all authors.

Additional Information

Supplementary information accompanies this paper at <https://doi.org/10.1038/s41598-018-20816-0>.

Competing Interests: The authors declare that they have no competing interests.

Publisher's note: Springer Nature remains neutral with regard to jurisdictional claims in published maps and institutional affiliations.



Open Access This article is licensed under a Creative Commons Attribution 4.0 International License, which permits use, sharing, adaptation, distribution and reproduction in any medium or format, as long as you give appropriate credit to the original author(s) and the source, provide a link to the Creative Commons license, and indicate if changes were made. The images or other third party material in this article are included in the article's Creative Commons license, unless indicated otherwise in a credit line to the material. If material is not included in the article's Creative Commons license and your intended use is not permitted by statutory regulation or exceeds the permitted use, you will need to obtain permission directly from the copyright holder. To view a copy of this license, visit <http://creativecommons.org/licenses/by/4.0/>.

© The Author(s) 2018